

# Small-Molecule Vasopressin-2 Receptor Antagonist Identified by a G-Protein Coupled Receptor “Pathway” Screen

Burane Yangthara, Aaron Mills, Varanuj Chatsudthipong, Lukmanee Tradtrantip, and A. S. Verkman

Departments of Medicine and Physiology, Cardiovascular Research Institute, University of California, San Francisco, California (B.Y., A.M., L.T., A.S.V.); and Department of Physiology, Faculty of Science, Mahidol University, Bangkok, Thailand (B.Y., V.C.)

Received January 25, 2007; accepted April 13, 2007

## ABSTRACT

G-protein-coupled receptors (GPCRs) such as the vasopressin-2 receptor ( $V_2R$ ) are an important class of drug targets. We developed an efficient screen for GPCR-induced cAMP elevation using as read-out cAMP activation of cystic fibrosis transmembrane conductance regulator (CFTR)  $Cl^-$  channels. Fischer rat thyroid cells expressing CFTR and a halide-sensing yellow fluorescent protein (H148Q/1152L) were transfected with  $V_2R$ . Increased cell  $Cl^-$  conductance after agonist-induced cAMP elevation was assayed using a plate reader from cell fluorescence after solution  $I^-$  addition. The  $Z'$  factor for the assay was  $\sim 0.7$  with the  $V_2R$  agonist [deamino-Cys1, Val4, D-Arg8]-vasopressin (1 nM) as positive control. Primary screening of 50,000 small molecules yielded a novel, 5-aryl-4-benzo-

yl-3-hydroxy-1-(2-arylethyl)-2H-pyrrol-2-one class of  $V_2R$  antagonists that are unrelated structurally to known  $V_2R$  antagonists. The most potent compound,  $V_2R_{inh-02}$ , which was identified by screening 35 structural analogs, competitively inhibited  $V_2R$ -induced cAMP elevation with  $K_i$  value of  $\sim 70$  nM and fully displaced radiolabeled vasopressin in binding experiments.  $V_2R_{inh-02}$  did not inhibit forskolin or  $\beta_2$ -adrenergic receptor-induced cAMP production and was more than 50 times more potent for  $V_2R$  than for  $V_{1a}R$ . The favorable in vitro properties of the pyrrol-2-one antagonists suggests their potential usefulness in aquaretic applications. The CFTR-linked cAMP assay developed here is applicable for efficient, high-throughput identification of modulators of cAMP-coupled GPCRs.

G-protein-coupled receptors (GPCRs) represent the largest and most versatile group of cell surface receptors (Hill, 2006). GPCRs are an important class of targets for the identification of clinically useful agonists and antagonists, constituting  $\sim 15\%$  of the total “druggable” genome and  $\sim 25\%$  of marketed drugs (Hopkins and Groom, 2002). GPCRs are coupled to the

G proteins  $G_s$  or  $G_i$ , which alter cAMP concentration, or  $G_q$ , which increases cytoplasmic calcium concentration. Of  $\sim 800$  GPCR genes identified in the human genome, 190 have known function (Wise et al., 2004), of which  $\sim 30$  are the targets of available drugs (Chalmers and Behan, 2002). The vasopressin-2 receptor ( $V_2R$ ) is of considerable interest because  $V_2R$  antagonists have aquaretic effects in the kidney for treatment of hyponatremias associated with inappropriately high levels of the antidiuretic hormone vasopressin (Schrier et al., 2006).

Several types of functional assays of cAMP concentration have been developed for high-throughput identification of modulators of  $G_s$ - or  $G_i$ -coupled GPCRs. The three available assay strategies include the following: 1) competition assay, which is based on competition between endogenous and radiolabeled cAMP for cAMP antibody binding

This work was supported by grants DK72517, DK35124, HL59198, EY13574, EB00415, and HL73856 from the National Institutes of Health, and Research Development Program (R613) and Drug Discovery grants from the Cystic Fibrosis Foundation (to A.S.V.). B.Y. is an MD-PhD student at Mahidol University, Bangkok, whose tenure in the Verkman laboratory was supported in part by a Royal Golden Jubilee grant PHD/0292/2545 from the Thailand research fund and by National Center for Genetic Engineering and Biotechnology (BIOTEC) Grant 3-2548, National Science and Technology Agency, Thailand.

Article, publication date, and citation information can be found at <http://molpharm.aspetjournals.org>.  
doi:10.1124/mol.107.034496.

**ABBREVIATIONS:** GPCR, G-protein-coupled receptor; CFTR, cystic fibrosis transmembrane conductance regulator; YFP, yellow fluorescent protein; AVP, arginine vasopressin; dDAVP, [deamino-Cys1, Val4, D-Arg8]-vasopressin;  $V_{1a}R$ , vasopressin-1a receptor;  $V_2R$ , vasopressin-2 receptor;  $V_{1b}R$ , vasopressin-1b receptor; FST, Fischer rat thyroid; HA, hemagglutinin; CHO, Chinese hamster ovary; PBS, phosphate-buffered saline; w, wild type; m, mutant; SR 49059, (2S)-1-(((2R,3S)-5-chloro-3-(o-chlorophenyl)-1-((3,4-dimethoxyphenyl)sulfonyl)-3-hydroxy-2-indolinyloxy)carbonyl)-2-pyrrolidinecarboxamide; SR 121463B, benzamide, N-(1,1-dimethylethyl)-4-((cis-5'-ethoxy-4-(2-(4-morpholinyl)ethoxy)-2'-oxospiro(cyclohexane-1,3'-(3H)indol)-1' (2'H)-yl)sulfonyl)-3-methoxy-, phosphate; OPC 21268, 1-(1-(4-(3-acetylamino-propoxy)benzoyl)-4-piperidyl)-3,4-dihydro-2(1H)-quinolinone; YM 087, (1,1'-biphenyl)-2-carboxamide, N-(4-(((4,5-dihydro-2-methylimidazo(4,5-d)1)benzazepin-6(1H)-yl)carbonyl)-phenyl)-, monohydrochloride; OPC 41061, (-)-4'-(7-chloro-2,3,4,5-tetrahydro-5-hydroxy-1H-1-benzazepin-1-yl)carbonyl)-o-tolu-m-toluidide; VPA 985, N-(3-chloro-4-(5H-pyrrolo(2,1-c)(1,4)benzodiazepin-10(11H)-ylcarbonyl)phenyl)-5-fluoro-2-methyl-benzamide.

(Williams, 2004); 2) reporter gene assay, in which cAMP drives the expression of a reporter gene containing a cAMP response element (Hill, 2001); and 3) cAMP-dependent protein activity assay, in which the cAMP-dependent activity of a target protein is measured (Rich and Karpen, 2005). The merits and limitations of these assays are described under *Discussion*. For G<sub>q</sub>-coupled GPCRs, assays of phosphatidylinositol, inositol triphosphate, and intracellular calcium have been developed (Horstman et al., 1988; Monteith and Bird, 2005).

In this study, we report an efficient assay of GPCR activity for G<sub>s</sub>- and G<sub>i</sub>-coupled GPCRs in which cAMP is assayed from halide conductance of the cystic fibrosis transmembrane conductance regulator (CFTR) protein. CFTR halide conductance is increased after cAMP-dependent phosphorylation mediated by protein kinase A. The principle of the assay is diagrammed in Fig. 1A. Cell expressing wild-type CFTR and a yellow fluorescent protein-based halide sensor (YFP-H148Q/I152L) are transfected with a GPCR. In the case of the G<sub>s</sub>-coupled GPCR V<sub>2</sub>R, agonist-induced cAMP elevation activates CFTR, which is assayed from the kinetics of I<sup>-</sup> entry into cells after solution I<sup>-</sup> addition. YFP-H148Q/I152L fluorescence is strongly quenched by I<sup>-</sup>, with 50% reduction in fluorescence at 2 to 3 mM I<sup>-</sup> (Galiotta et al., 2001a). We reported previously that Fischer rat thyroid (FRT) cells express CFTR and YFP strongly and stably after transfection and have other properties suitable for high-throughput screening, including low basal halide transport, rapid growth on plastic, and high electrical resistance (Galiotta et al., 2001b). FRT cells expressing YFPs and wild-type or mutant CFTRs were used by our lab to identify CFTR activators for potential treatment of cystic fibrosis (Pedemonte et al., 2005) and CFTR inhibitors for potential therapy of secretory diarrheas and polycystic kidney disease (Ma et al., 2002; Muangprasat et al., 2004). Here we validate the CFTR-linked GPCR assay as applied to the identification of V<sub>2</sub>R antagonists and

report the discovery and characterization of a 5-aryl-4-benzoyl-3-hydroxy-1-(2-arylethyl)-2H-pyrrol-2-one class of V<sub>2</sub>R antagonists.

## Materials and Methods

**Plasmids.** Plasmids encoding human wild-type and mutant (W164S) V<sub>2</sub>R were kindly provided by Dr. Daniel Bichet (University of Montreal, Montreal, QC, Canada). N-terminal c-myc-tagged V<sub>2</sub>R were created by polymerase chain reaction introduction of a c-myc sequence after the methionine initiation sequence. Polymerase chain reaction products were subcloned into plasmid pCDNA3.1Hyg+ (Invitrogen, Carlsbad, CA) at XbaI and HindIII restriction sites to give plasmids wV<sub>2</sub>R-Hyg (wild type) and mV<sub>2</sub>R-Hyg (mutant). cDNAs were confirmed by sequence analysis. The pCDNA3.1 plasmids encoding HA-tagged human  $\beta$ -adrenergic and vasopressin V<sub>1a</sub> receptors were purchased from the University of Missouri–Rolla cDNA Resource Center.

**Cell Culture and Transfection.** Fisher rat thyroid cells expressing CFTR and YFP-H148Q/I152L, as described previously (Muangprasat et al., 2004), CHO-K1 cells, and Calu-3 cells were cultured in F-12 modified Coon's medium (Sigma, St. Louis, MO), F-12 Ham's Nutrient mix, and minimal essential Eagle's medium and Earle's balanced salt solution medium, respectively. Media were supplemented with 10% fetal bovine serum, 100 U/ml penicillin, and 100  $\mu$ g/ml streptomycin. The medium for FRT cells was supplemented with 2 mM glutamine, 500  $\mu$ g/ml Zeocin, and 500  $\mu$ g/ml Geneticin. The medium for Calu-3 cells was supplemented with 2 mM glutamine, 0.11 mg/ml sodium pyruvate, 1.5 g/l NaHCO<sub>3</sub>, and nonessential amino acids. Cells were grown at 37°C in 5% CO<sub>2</sub>/95% air.

For stable transfection, cells at ~80% confluence were transfected with wV<sub>2</sub>R-Hyg, HA-tagged human V<sub>1a</sub>R, or mV<sub>2</sub>R-Hyg using Lipofectamine 2000 (Invitrogen) according to manufacturer's instructions. Twenty-four hours after transfection, the cells were selected for 2 weeks with 350  $\mu$ g/ml hygromycin (Roche, Indianapolis, IN) for V<sub>2</sub>R or with 750  $\mu$ g/ml Geneticin (Invitrogen) for V<sub>1a</sub>R. Remaining colonies were grown at clonal density and screened for receptor expression by immunofluorescence and immunoblot analysis. Stably transfected cell lines were maintained in the same medium used for selection. Transient transfection of CHO-K1 cells with the HA-tagged human  $\beta$ -adrenergic receptor was done in a manner similar to the stable transfections. Cells were used 48 h after transient transfection.

**Immunofluorescence and Immunoblot Analysis.** For c-myc immunostaining, nonpermeabilized cells were washed three times with phosphate-buffered saline (PBS) and incubated for 1 h with anti-c-myc antibody (1:1000; Roche) in PBS containing 1% bovine serum albumin, washed three times with PBS, and fixed for 10 min in 4% paraformaldehyde. After three washes with PBS, cells were incubated for 1 h with Cy3-conjugated anti-rabbit IgG (Zymed Laboratories, South San Francisco, CA), washed, and mounted for fluorescence microscopy. Immunostaining of permeabilized cells was done similarly, except that cells were permeabilized with 0.1% Triton X-100 in PBS before fixation and blocked for 15 min in PBS containing 1% bovine serum albumin.

For immunoblot, cells were homogenized in 250 mM sucrose, 1 mM EDTA, and 1% protease inhibitor cocktail (Sigma). The homogenate was centrifuged at 5000g for 10 min, and the supernatant was assayed for protein concentration (Bio-Rad DC kit; Bio-Rad, Hercules, CA). Proteins (20  $\mu$ g/lane) were resolved by SDS-polyacrylamide gel electrophoresis (NuPAGE 4–12% Bis-Tris gel; Invitrogen) and transferred to a polyvinylidene difluoride membrane. The polyvinylidene difluoride membrane was blocked overnight in 5% skim milk in PBS containing 1% Tween 20, washed three times, and incubated for 2 h with anti-c-myc antibody (1:1000). The membrane was then washed three times, incubated for 1 h with horseradish peroxidase-conjugated anti-rabbit IgG (Cell Signaling Technology,

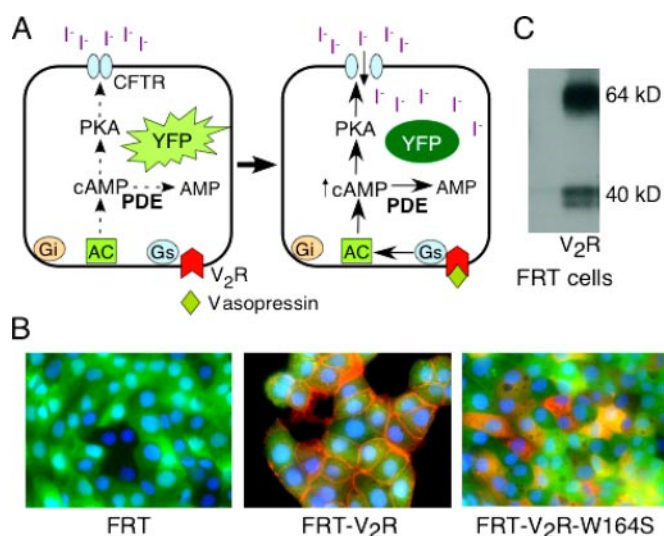


**Fig. 1.** Assay and cell lines used for V<sub>2</sub>R antagonist screening. A, principle of the assay, showing increased I<sup>-</sup> influx after cAMP activation of plasma membrane CFTR Cl<sup>-</sup> channels. B, staining of nontransfected FRT cells (FRT), FRT cells stably expressing wild-type human V<sub>2</sub>R (FRT-V<sub>2</sub>R), and FRT cells stably expressing the W164S mutant of V<sub>2</sub>R (FRT-V<sub>2</sub>R-W164S). Anti-c-myc staining is shown in red, with YFP in green and nuclei (4,6-diamidino-2-phenylindole) in blue. C, immunoblot of a crude protein extract from FRT (left lane) and FRT-V<sub>2</sub>R (right lane) cells.

Danvers, MA), washed, and detected by enhanced chemiluminescence (GE Healthcare, Chalfont St. Giles, Buckinghamshire, UK).

**YFP Fluorescence Measurement of I<sup>-</sup> Influx.** Transfected FRT cells were plated in black-walled, 96-well plates with transparent plastic bottom (Corning-Costar, Acton, MA), cultured overnight to confluence, washed three times with PBS, and treated with specified compounds in a final volume of 60  $\mu$ l. YFP-H148Q/I152L fluorescence was measured using a commercial plate reader (FluoStar Optima; BMG LabTechnologies, Offenburg, Germany) equipped with custom excitation and emission filters (500 nm and 544 nm, respectively; Chroma, Brattleboro, VT). Fluorescence intensity in each well was measured for a total of 14 s. In each well, 100  $\mu$ l of PBS/I<sup>-</sup> (PBS with 100 mM Cl<sup>-</sup> replaced by I<sup>-</sup>) was injected by a syringe pump at 2 s after the start of data collection.

**CFTR Cl<sup>-</sup> Current Measurement.** Cells were cultured on Snapwell filters (Costar 3801) until confluence (transepithelial resistance, >500  $\Omega$ ). Apical membrane current was measured in an Ussing chamber (Vertical diffusion chamber; Costar) with Ringer's solution bathing the basolateral surface and half-Ringer's bathing the apical surface. The composition of Ringer's solution was 130 mM NaCl, 2.7 mM KCl, 1.5 mM KH<sub>2</sub>PO<sub>4</sub>, 1 mM CaCl<sub>2</sub>, 0.5 mM MgCl<sub>2</sub>, 10 mM sodium HEPES, and 10 mM glucose, pH 7.3. Half-Ringer's solution was the same, except that 65 mM NaCl was replaced with sodium gluconate, and CaCl<sub>2</sub> was increased to 2 mM. Chambers were bubbled continuously with air. Apical membrane current was measured using a DVC-1000 voltage-clamp apparatus (World Precision Instruments, Sarasota, FL).

**High-Throughput Screening.** The compound library for screening contained 50,000 chemically diverse, drug-like small molecules (ChemDiv, San Diego, CA). Stock compounds were stored in 96-well plates at 2.5 mM in dimethyl sulfoxide. Compounds occupied 80 wells, with the remaining 16 wells containing only dimethyl sulfoxide (for positive and negative controls). Screening was done using an automated apparatus (Beckman Coulter, Fullerton, CA) containing a CO<sub>2</sub> incubator, carousels for compound plates and pipette tip boxes, plate washer (Elx405; Bio-Tek Instruments, Winooski, VT), liquid handling station (Biomek FX; Beckman Coulter), and two plate readers (FluoStar Optima; BMG LabTechnologies). Robotic operations were controlled by SAMI software (version 3.3; Beckman Coulter).

For high-throughput screening, cells expressing human wild-type V<sub>2</sub>R were plated in 96-well plates using a LabSystems Multidrop Dispenser. After overnight growth to confluence, cells were washed with PBS, and dDAVP (1 nM; Ferring Pharmaceuticals, Suffern, NY) was added together with test compounds (20  $\mu$ M). The first and last columns of each plate were used for positive (PBS) and negative (dDAVP, no test compound) controls. I<sup>-</sup> influx was assayed as described above after a 30-min incubation at 37°C in a CO<sub>2</sub> incubator.

**Data Analysis.** I<sup>-</sup> influx (d[I<sup>-</sup>]/dt at  $t = 0$ ) was computed from fluorescence time course data as described previously (Muanprasat et al., 2004). Percentage of inhibition was computed using the following equation: % inhibition = 100  $\times$  (negative control - compound)/(negative control - positive control). Positive and negative control values denote d[I<sup>-</sup>]/dt obtained from the first and last columns of each plate. Primary screening data were subjected to histogram analysis for "hit" selection.

**Synthesis Procedures.** To synthesize 2,4-dioxo-4-phenyl-ethyl-butylate **1**, a solution of anhydrous benzene (50 ml) and acetophenone (1.2 g, 0.010 mol) was added to a suspension of NaH in oil (60%; 0.8 g, 0.020 mol), and the mixture was stirred for 30 min. To a solution of diethyl oxalate (2.19 g, 0.015 mol), benzene (10 ml) was added drop-wise, and the reaction mixture was stirred for 6 h. The mixture was filtered over Celite and purified by chromatography to give 2,4-dioxo-4-phenyl-ethylbutylate **1** (1.76 g; 85% yield). To synthesize 4-benzoyl-5-(4-fluorophenyl)-3-hydroxy-1-(4-hydroxyphenylethyl)-2,5-dihydro-2-pyrrolone (V<sub>2</sub>R<sub>inh-02</sub>), tyramine (93 mg, 0.675 mmol) and 4-fluorobenzaldehyde (84 mg, 0.675 mmol) were heated to 110°C for 10 min. Water was removed during reflux with a cotton

swab. Compound **1** (135 mg, 0.614 mmol) was added drop-wise in dioxane (5 ml) and stirred overnight at 100°C. The 2-pyrrolone was purified by column chromatography and recrystallized to give V<sub>2</sub>R<sub>inh-02</sub> (153 mg, 60% yield). <sup>1</sup>H NMR (400 MHz, CD<sub>3</sub>OD):  $\delta$  7.72 (d,  $J = 7.6$  Hz, 2H), 7.59 (t,  $J = 7.2$  Hz, 1H), 7.48 (d, 8.0 = Hz, 2H), 7.24 (m, 2H), 7.10 (t,  $J = 8.8$  Hz, 1H), 7.03 (d,  $J = 8.6$  Hz, 2H), 6.81 (d,  $J = 8.6$  Hz, 2H), 5.26 (s, 1H), 3.91 (m, 1H), 3.36 (s, 1H), 2.97 to 2.68 (m, 2H), 2.71 (m, 1H). Liquid chromatography-mass spectrometry:  $m/z$  418.1 [M + H]<sup>+</sup> (C<sub>18</sub> column, 99%, 200–400 nm; Nova-Pak, Eatontown, NJ).

**cAMP Measurement.** Cells were grown in 24-well plates, treated with test compounds for 30 min, lysed by sonication, centrifuged to remove cell debris, and assayed for cAMP according to manufacturer's instructions (R&D Systems, Minneapolis, MN). For CHO-K1 cells, 24 h after transfection with  $\beta_2$ -adrenergic receptors, cells were trypsinized and plated onto 24-well plates overnight before cAMP assay.

**Receptor Binding Assay.** Radiolabeled vasopressin binding was measured in intact FRT cells stably expressing human V<sub>2</sub>R or V<sub>1a</sub>R. Confluent cells in 24-well plates were washed twice with ice-cold binding buffer (PBS containing 0.1% glucose and 0.2% bovine serum albumin). Cells were incubated for 2 h at 4°C with binding buffer containing 1 nM [<sup>3</sup>H]AVP (PerkinElmer Life and Analytical Sciences, Boston, MA) and specified concentrations of V<sub>2</sub>R<sub>inh-02</sub>, washed twice with ice-cold PBS, and lysed in 0.1 N NaOH containing 0.2% SDS. Radioactivity was measured with a scintillation counter. Nonspecific binding, determined by radioactivity with dDAVP (for V<sub>2</sub>R) or SR 49059 (for V<sub>1a</sub>R) incubation, was subtracted. dDAVP and SR 49059 (Sanofi Aventis, Montpellier, France) bind selectively to V<sub>2</sub>R and V<sub>1a</sub> receptor, respectively (Serradeil-Le Gal et al., 1993).

## Results

**Expression of the Wild-Type and the Mutant V<sub>2</sub>Rs in FRT Cells.** Stably transfected FRT cell lines were generated that coexpress human wild-type CFTR, YFP-H148Q/I152L, and c-myc-tagged wild-type V<sub>2</sub>R or the mutant V<sub>2</sub>R-W164S. The c-myc-tag was inserted at the external-facing V<sub>2</sub>R N terminus. Wild-type V<sub>2</sub>R showed a plasma membrane distribution by c-myc staining (Fig. 1B), whereas no membrane staining was seen in nontransfected cells or cells expressing V<sub>2</sub>R-W164S that has a defect in cellular processing with retention at the endoplasmic reticulum (Oksche et al., 1996). Immunoblot analysis with c-myc antibody showed bands at ~40 and 64 kDa, corresponding to nonglycosylated and glycosylated V<sub>2</sub>R, respectively (Innamorati et al., 1996; Sadeghi et al., 1997). These results indicate stable surface expression of wild-type V<sub>2</sub>R in FRT cells.

Forskolin, an adenylyl cyclase activator, and dDAVP, a V<sub>2</sub>R-selective vasopressin receptor agonist (Chang et al., 2005), increase cytoplasmic cAMP concentration and hence activate CFTR. CFTR activity was assayed from the kinetics of decreasing YFP-H148Q/I152L fluorescence after external I<sup>-</sup> addition. Forskolin treatment increased CFTR activity in wild-type, mutant, and nontransfected cells, whereas dDAVP increased CFTR activity only in cells expressing wild-type V<sub>2</sub>R (Fig. 2A). Increased CFTR activity in response to forskolin or dDAVP was inhibited by the CFTR blocker CFTR<sub>inh-172</sub> (Ma et al., 2002). Inhibition of dDAVP-stimulated I<sup>-</sup> influx was found with the partial V<sub>2</sub>R agonist [1- $\beta$ -mercapto- $\beta$ ,  $\beta$ -cyclopentamethylenepropionyl<sup>1</sup>, O-ET-TYR<sup>2</sup>, VAL<sup>4</sup>, ARG<sup>8</sup>]-vasopressin (Sigma) and the V<sub>2</sub>R antagonist SR 121463B (Sanofi Pharmaceutical) (Serradeil-Le Gal et al., 1996; Manning et al., 1997). Concentration-activation data are summarized in Fig. 2B. The IC<sub>50</sub> value for CFTR activation by dDAVP of ~0.1 nM is less than that observed in V<sub>2</sub>R

radioligand binding experiments but is comparable with that reported in other functional assays (Saito et al., 1997). Figure 2C shows the forskolin and dDAVP concentration-dependent increase in apical membrane Cl<sup>-</sup> current in FRT cells expressing wild-type V<sub>2</sub>R, providing a direct measure of CFTR function. In each case, the current was fully inhibited by CFTR<sub>inh</sub>-172. These results confirm functional cell surface expression of wild-type V<sub>2</sub>R in the stably transfected FRT cells.

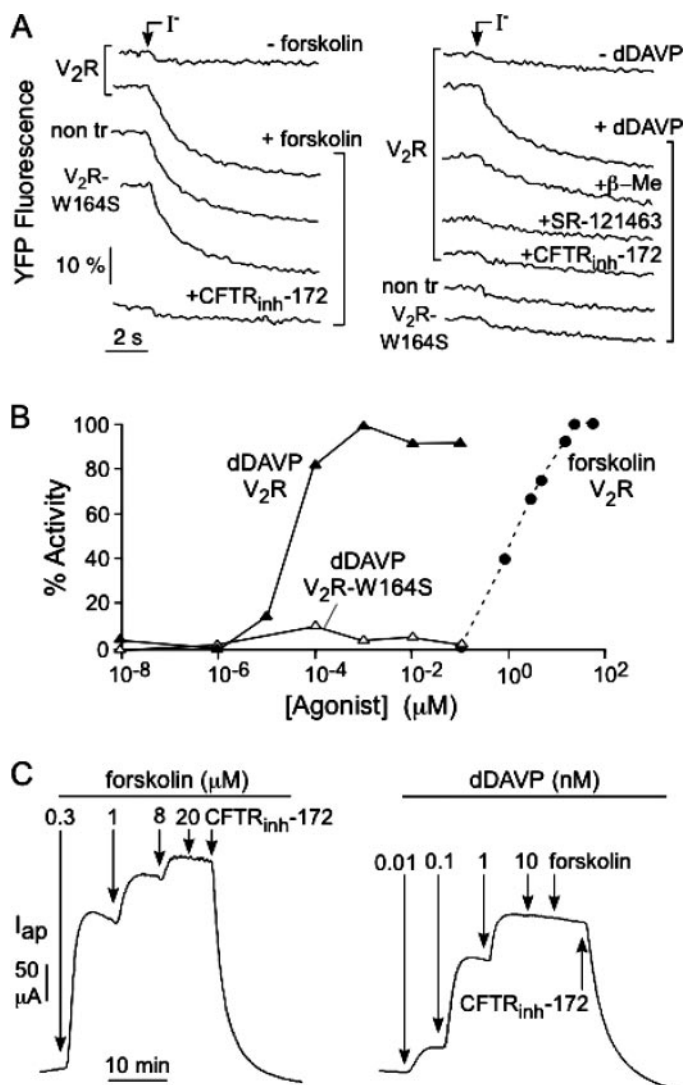


**Fig. 2.** Functional characterization of FRT-V<sub>2</sub>R-expressing FRT cells. **A**, YFP fluorescence after I<sup>-</sup> addition in FRT, FRT-V<sub>2</sub>R, and FRT-V<sub>2</sub>R-W164S cells. Cells were preincubated with 20 μM forskolin (left) or 1 nM dDAVP (right) for 20 min before I<sup>-</sup> addition. Indicated inhibitors were present before and during measurements: CFTR<sub>inh</sub>-172 (20 μM); [1-β-mercapto-β, β-cyclopentamethylenepropionyl<sup>1</sup>, O-ET-TYR<sup>2</sup>, VAL<sup>4</sup>, ARG<sup>8</sup>]-vasopressin (β-ME, 10 μM); and SR 121463B (10 μM). The scale bar on the y-axis indicates the percentage of fluorescence reduction relative to baseline fluorescence (before iodide addition). Curves were displaced in the y-axis direction for clarity. **B**, percentage of maximal activity (from initial fluorescence slopes after I<sup>-</sup> addition) as a function of forskolin and dDAVP concentrations in FRT-V<sub>2</sub>R and FRT-V<sub>2</sub>R-W164S cells. The percentage of maximal activity was a percentage of cellular response to an agonist relative to the maximal response triggered by the same agonist. The data reflected findings in a single well experiment (**C**). Forskolin and dDAVP concentration-response data in FRT-V<sub>2</sub>R cells measured as apical membrane current (*I*<sub>ap</sub>) in short-circuit current measurements. Where indicated, 20 μM CFTR<sub>inh</sub>-172 was added.

**High-Throughput Screening.** To establish a screening assay using the V<sub>2</sub>R-transfected cells, we first investigated the possible effects of agonist-induced receptor desensitization/internalization, which for GPCRs depends on incubation time and agonist concentration (Robben et al., 2004). Figure 3A shows incubation time- and concentration-dependent reduction in the cellular response to dDAVP, as assayed by CFTR activation. At 1 μM dDAVP, the response was maximal but decreased rapidly with time. Similar maximal responses were found for 1 and 10 nM dDAVP but with little time-dependent desensitization. For primary screening, we used 1 nM dDAVP to maximize sensitivity for the detection of weakly active, small-molecule competitive antagonists. To prove that receptor desensitization rather than downstream processes was responsible for the time-dependent reduced response to dDAVP, a similar study was done using a high concentration of forskolin in place of dDAVP. Forskolin (100

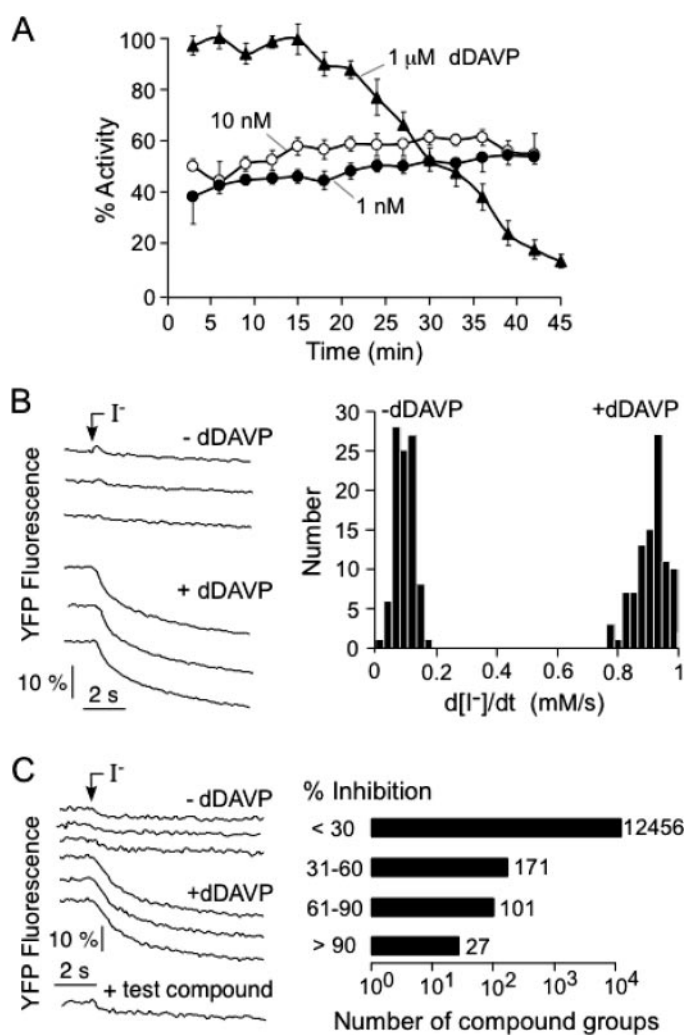


**Fig. 3.** Validation of the screening assay for identification of V<sub>2</sub>R antagonists. **A**, time course of V<sub>2</sub>R desensitization assayed by I<sup>-</sup> influx in FRT-V<sub>2</sub>R cells exposed to indicated dDAVP concentrations. The data are shown as mean ± S.E. (*n* = 4). **B**, left, YFP fluorescence of FRT-V<sub>2</sub>R cells preincubated with 0 or 1 nM dDAVP for 30 min with I<sup>-</sup> added as indicated. Right, histogram distribution of I<sup>-</sup> influx (*d*[I<sup>-</sup>]/*dt*) determined from initial fluorescence slopes. **C**, left, examples of positive and negative control fluorescence data from individual wells in the primary screen and an example of an active test compound. Right, histogram distribution of the percentage of inhibition from screening of 50,000 small molecules in groups of 4.

$\mu\text{M}$ ) fully activated CFTR but without a measurable reduction in activity over 45 min, supporting a desensitization mechanism for dDAVP.

The suitability of the assay for high-throughput screening was evaluated by experimental determination of the  $Z'$  factor, a quantitative measure of assay "goodness" that depends on the difference in positive and negative control signals and their standard deviations (Seethala and Fernandes, 2001). Figure 3B (left) shows original fluorescence data from individual wells of 96-well plates incubated for 30 min with PBS or 1 nM dDAVP. The distribution of  $\text{I}^-$  influx rates in individual wells,  $d[\text{I}^-]/dt$ , shows well-separated positive and negative controls (Fig. 3B, right), giving a  $Z'$  factor of 0.71. A  $Z'$  factor greater than 0.5 to 0.6 is considered excellent such that a single primary screen is predicted to be informative in identifying "hits." Test compounds did not quench YFP-H148Q/I152L fluorescence directly as indicated by similar cell fluorescence before  $\text{I}^-$  addition.

A primary screen of 50,000 small molecules was done using the FRT cells expressing wild-type human  $\text{V}_2\text{R}$ , CFTR and YFP-H148Q/I152L. Cells were incubated with 1 nM dDAVP and test compounds (20  $\mu\text{M}$  final concentration) for 30 min before fluorescence assay of  $\text{I}^-$  influx. Figure 3C (left) shows representative original data for positive and negative controls, along with an example of an active test compound. Figure 3C (right) summarizes the percentage inhibition values as a frequency histogram. The majority of the compound groups (12,456 groups of 4 different compounds) did not reduce  $d[\text{I}^-]/dt$  (<30% inhibition at 20  $\mu\text{M}$ ). Two hundred seventy-two compound groups were classified as weak inhibitors (30–90% inhibition), and 27 groups were considered strong inhibitors (> 90% inhibition). These definitions of weak versus strong inhibitors are arbitrary.

The "strong" inhibitor groups identified in the primary screen were further evaluated to confirm their inhibition activity at low micromolar concentration and to identify individual compounds responsible for activity out of the groups-of-four used in the primary screen. Approximately 70% of the hits identified in the primary screen were confirmed in subsequent secondary screening by the fluorescence plate reader assay. Three potent classes of compounds were found, one of which was a  $\text{V}_2\text{R}$  antagonist (Fig. 4A), as judged by selective inhibition of dDAVP-induced cAMP production (see below). The  $\text{V}_2\text{R}$  antagonist is of the 5-aryl-4-benzoyl-3-hydroxy-1-(2-arylethyl)-2H-pyrrol-2-one chemical class, which is not structurally similar to known  $\text{V}_2\text{R}$  antagonists (OPC 31260 and SR 121463A structures shown in Fig. 4A). The other (non- $\text{V}_2\text{R}$  antagonist) hits identified in the screen are being characterized and are not discussed further in this article. These compounds inhibited forskolin-induced cellular responses; thus, they act at downstream sites.

**Analysis of Structure-Activity Relationship.** Structure-activity relationship analysis was done by screening a small set of 81 commercially available 2,5-dihydro-2-pyrrolone analogs. Table 1 lists  $\text{V}_2\text{R}$  inhibition data of active compounds, and Fig. 4B (left) summarizes the structure-activity relationship analysis in terms of the functional groups conferring  $\text{V}_2\text{R}$  antagonist activity. At position  $\text{R}_1$ , phenyl and 4-substituted phenyl conferred greatest inhibition; inhibition was lost when  $\text{R}_1$  was methyl or furanyl. It is noteworthy that  $\text{V}_2\text{R}_{\text{inh}}-13$ , which contains a thiophenyl ring at  $\text{R}_1$ , was also active. The greatest diversity in the collection of 2-pyrrolone

analog was in  $\text{R}_2$ . Activity was seen primarily for 4-halogeno or 4-nitro-substituted phenyl. Exceptions to this were the two 2-fluorophenyl derivatives [ $\text{V}_2\text{R}_{\text{inh}}-04$  and  $\text{V}_2\text{R}_{\text{inh}}-11$ ] and the 3-nitrophenyl derivative [ $\text{V}_2\text{R}_{\text{inh}}-08$ ]. Phenyl substitutions at  $\text{R}_2$  that led to inactive compounds were generally electron-donating substituents, including methoxy, hydroxy, and alkyl; exceptions to this were the two 4-methoxyphenyl derivatives [ $\text{V}_2\text{R}_{\text{inh}}-03$  and  $\text{V}_2\text{R}_{\text{inh}}-07$ ]. Methyl formate esters and other heterocycles were not tolerated at  $\text{R}_2$ , including furyl, thiophenyl, and 3-pyridinyl rings.  $\text{R}_3$  as phenyl and 4-hydroxy phenyl gave active compounds; 3,4-dimethoxyphenyl and 4-hydroxy-3-methoxyphenyl analogs were inactive. The 4-hydroxyphenyl derivative gave the greatest inhibition potency, with the most potent compound being  $\text{V}_2\text{R}_{\text{inh}}-02$ . This compound was synthesized in pure form on a large scale and further characterized.

**Synthesis and Characterization of  $\text{V}_2\text{R}_{\text{inh}}-02$ .** The synthesis of  $\text{V}_2\text{R}_{\text{inh}}-02$  was accomplished in two steps. The dioxoethyl butylate **1** was synthesized by reaction of the enolate of acetophenone with diethoxyethylate to give 2,4-dioxo-

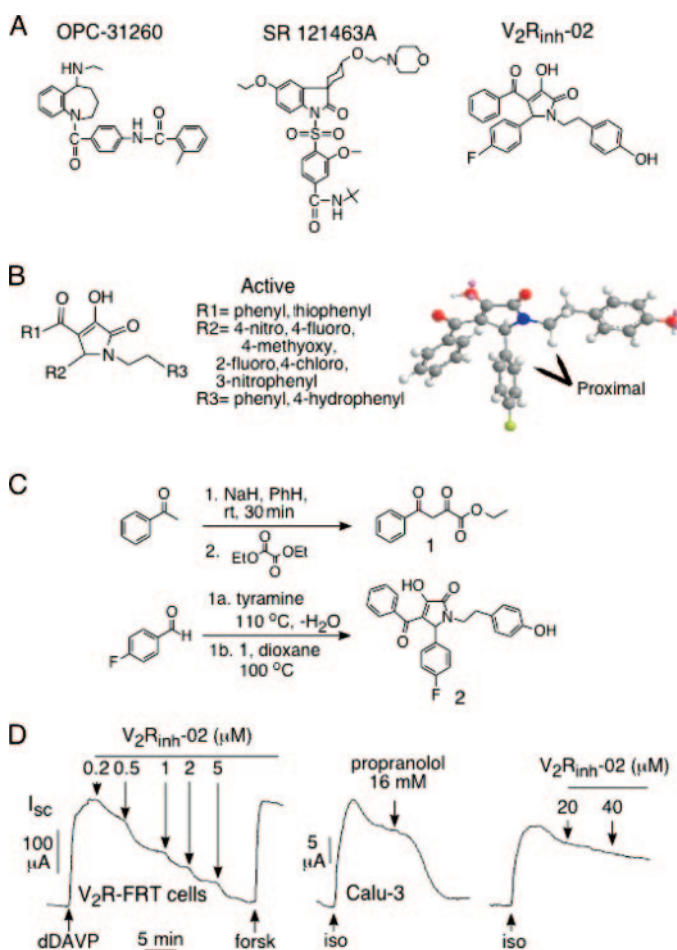


**Fig. 4.** Structure-activity of  $\text{V}_2\text{R}$  antagonists. A, Structure of  $\text{V}_2\text{R}_{\text{inh}}-02$  shown with previously identified  $\text{V}_2\text{R}$  antagonists OPC 312260 and SR 121463A. B, summary of structure-activity relationship data for 35 compounds (left) (see Table 1). Right, Predicted three-dimensional structure of  $\text{V}_2\text{R}_{\text{inh}}-02$ . C, Synthesis of  $\text{V}_2\text{R}_{\text{inh}}-02$  (see text for description). D, left, concentration-dependence data for  $\text{V}_2\text{R}_{\text{inh}}-02$  inhibition of apical membrane CFTR  $\text{Cl}^-$  current in  $\text{V}_2\text{R}$ -expressing FRT cells after activation by 1 nM dDAVP. Where indicated, 20  $\mu\text{M}$  forskolin was added. Center and right, inhibition of isoproterenol-stimulated short-circuit current in Calu-3 cells by indicated concentrations of propranolol and  $\text{V}_2\text{R}_{\text{inh}}-02$ .

4-phenyl-ethylbutylate **1** (Fig. 4C). After reaction of 4-bromobenzaldehyde and tyramine to form the imine, the addition of 2,4-dioxo-4-phenyl-ethylbutylate **1** in dioxane gave V<sub>2</sub>R<sub>inh</sub>-02 (Fig. 4C), which was purified by crystallization. Its pK<sub>a</sub> value was 4.76, as measured by spectrophotometric titration (absorbance 346 nm) of 100 μM V<sub>2</sub>R<sub>inh</sub>-02 in aqueous solution containing citric acid, sodium acetate, HEPES, sodium borate, Tris, and sodium carbonate (each 5 mM) titrated to indicated pH using HCl and NaOH. Deprotonation of the hydroxyl group on the pyrrolone ring occurs at low pH, such that V<sub>2</sub>R<sub>inh</sub>-02 contains a single negative charge at physiological pH. The aqueous solubility of V<sub>2</sub>R<sub>inh</sub>-02 in PBS was 377 μM as measured by optical absorbance of a saturated solution after appropriate dilution. The high aqueous solubility of V<sub>2</sub>R<sub>inh</sub>-02 is a consequence of its polarity and charge.

V<sub>2</sub>R<sub>inh</sub>-02 identity was confirmed by <sup>1</sup>H NMR and mass spectrometry. Purity was determined to be 99% by liquid chromatography. Figure 4B (right) shows the predicted three-dimensional structure of V<sub>2</sub>R<sub>inh</sub>-02 based on energy minimization computations. An interesting finding from <sup>1</sup>H NMR spectra was the magnetic nonequivalence of the two CH<sub>2</sub> groups of the 1-(4-hydroxyphenethyl) fragment. From the computed structure, we conclude that this magnetic nonequivalence is due to the proximal 4-fluorophenyl group interacting with the hydrogen on the -CH<sub>2</sub>-N group, accounting for the AA'BB' splitting pattern and the downfield chemical shift ~3.9 ppm of the proximal proton. This interpretation is supported by published structure data for 5-aryl-1-benzyl-2,5-dihydro-2-pyrrolones (Aliiev et al., 2003).

V<sub>2</sub>R<sub>inh</sub>-02 was first tested for its inhibitory potency in apical membrane current measurements of CFTR Cl<sup>-</sup> channel activity. Figure 4D, which is representative of three separate experiments, shows V<sub>2</sub>R<sub>inh</sub>-02 concentration-dependent inhibition of Cl<sup>-</sup> current induced by 1 nM dDAVP, with an IC<sub>50</sub> value of 0.5 ± 0.1 μM (mean ± S.D., n = 3).

Several possible steps in the signal transduction cascade for CFTR activation could be modulated by V<sub>2</sub>R<sub>inh</sub>-02, including the following: 1) V<sub>2</sub>R; 2) G-proteins, G<sub>s</sub> or G<sub>i</sub>; 3) adenylyl cyclase; 4) phosphodiesterase; 5) protein kinase A; and 6) CFTR. The failure of V<sub>2</sub>R<sub>inh</sub>-02 to inhibit forskolin-induced Cl<sup>-</sup> current, as seen in Fig. 4D (left), indicates that V<sub>2</sub>R<sub>inh</sub>-02 is unlikely to act on G<sub>i</sub>, adenylyl cyclase, or more distal components of the signal transduction cascade. To distinguish the action of V<sub>2</sub>R<sub>inh</sub>-02 as a V<sub>2</sub>R antagonist versus a G<sub>s</sub> inhibitor, short-circuit current was measured in Calu-3 cells,

which natively express the β<sub>2</sub>-adrenergic G<sub>s</sub>-coupled receptor. Figure 4D (center) shows inhibition of isoproterenol-induced short-circuit current in Calu-3 cells by the β<sub>2</sub> antagonist propranolol. V<sub>2</sub>R<sub>inh</sub>-02 did not inhibit the isoproterenol-induced response in Calu-3 cells (Fig. 4D, right). Together, these findings suggest that V<sub>2</sub>R<sub>inh</sub>-02 is a V<sub>2</sub>R antagonist.

Measurements of cAMP concentration were made in the V<sub>2</sub>R-expressing FRT cells to verify the action of V<sub>2</sub>R<sub>inh</sub>-02 at the vasopressin-2 receptor. Figure 5A (left) shows dDAVP concentration-response data for the elevation of cAMP concentration. V<sub>2</sub>R<sub>inh</sub>-02 inhibition of cAMP concentration after stimulation by 1 nM dDAVP is shown in Fig. 5A (right). The IC<sub>50</sub> value was ~60 nM. To verify the action of V<sub>2</sub>R<sub>inh</sub>-02 on the V<sub>2</sub>R, cAMP concentration was measured in β<sub>2</sub> receptor-transfected CHO cells (Fig. 5B). Cellular cAMP was increased by isoproterenol, as expected. The increased cAMP concentration was inhibited by propranolol but not by SR 121463B or V<sub>2</sub>R<sub>inh</sub>-02, supporting V<sub>2</sub>R inhibition by V<sub>2</sub>R<sub>inh</sub>-02.

**V<sub>2</sub>R<sub>inh</sub>-02 Is a Competitive V<sub>2</sub>R Antagonist.** Figure 6A shows a functional “competition study” in which V<sub>2</sub>R<sub>inh</sub>-02 reduction of cAMP concentration was measured in V<sub>2</sub>R-expressing FRT cells after stimulation by different concentrations of dDAVP. The dDAVP dose-response curves shifted in a parallel manner to the right with increasing V<sub>2</sub>R<sub>inh</sub>-02 concentration, indicative of a competitive binding mechanism. A Schild plot is shown in the inset to Fig. 6A, in which [V<sub>2</sub>R<sub>inh</sub>-02] is plotted against the dDAVP dose ratio (Kenakin, 1997). The slope of 1.3 of the fitted line supports a competitive inhibition mechanism with a K<sub>i</sub> value of ~70 nM.

Binding displacement assays were done to prove V<sub>2</sub>R<sub>inh</sub>-02 competition with vasopressin at the V<sub>2</sub>R. Cell-associated radiolabeled vasopressin was measured after binding to V<sub>2</sub>R-expressing FRT cells. The V<sub>2</sub>R-selective binding component was determined by subtracting cell-associated radioactivity in the presence of a high concentration of nonradioactive dDAVP. As summarized in Fig. 6B, V<sub>2</sub>R<sub>inh</sub>-02 at 1 μM reduced cell-associated radioactivity to near 0 with 50% competition at ~70 nM, supporting a competitive V<sub>2</sub>R<sub>inh</sub>-02 binding mechanism. To investigate V<sub>2</sub>R versus V<sub>1a</sub>R binding selectivity, similar binding displacement experiments were done in FRT cells stably expressing V<sub>1a</sub>R. Fifty percent competition of V<sub>2</sub>R<sub>inh</sub>-02 to [<sup>3</sup>H]AVP was seen at ~5 μM (Fig. 6B), indicating ~70 times greater affinity of V<sub>2</sub>R<sub>inh</sub>-02 to V<sub>2</sub>R than V<sub>1a</sub>R.

TABLE 1  
Structure-activity relationships of active V<sub>2</sub>R antagonists

Compound	R1	R2	R3	Inhibition at 20 μM
				%
V <sub>2</sub> R <sub>inh</sub> -01	Ph	4-NO <sub>2</sub> -Ph	Ph	20
V <sub>2</sub> R <sub>inh</sub> -02	Ph	4-F-Ph	4-OH-Ph	100
V <sub>2</sub> R <sub>inh</sub> -03	4-Me-Ph	4-OMe-Ph	Ph	50
V <sub>2</sub> R <sub>inh</sub> -04	4-OMe-Ph	2-F-Ph	Ph	41
V <sub>2</sub> R <sub>inh</sub> -05	4-OMe-Ph	4-Cl-Ph	Ph	82
V <sub>2</sub> R <sub>inh</sub> -06	4-OMe-Ph	4-NO <sub>2</sub> -Ph	Ph	10
V <sub>2</sub> R <sub>inh</sub> -07	4-OMe-Ph	4-OMe-Ph	Ph	45
V <sub>2</sub> R <sub>inh</sub> -08	4-Cl-Ph	3-NO <sub>2</sub> -Ph	Ph	40
V <sub>2</sub> R <sub>inh</sub> -09	4-Cl-Ph	4-NO <sub>2</sub> -Ph	Ph	60
V <sub>2</sub> R <sub>inh</sub> -10	4-Br-Ph	2-F-Ph	Ph	71
V <sub>2</sub> R <sub>inh</sub> -11	4-Br-Ph	4-Cl-Ph	Ph	72
V <sub>2</sub> R <sub>inh</sub> -12	4-Br-Ph	4-NO <sub>2</sub> -Ph	Ph	35
V <sub>2</sub> R <sub>inh</sub> -13	Thiophenyl	4-Cl-Ph	Ph	62

Ph, phenyl; Br, bromo; Cl, chloro; F, fluoro; OMe, methoxy; NO<sub>2</sub>, nitro.

## Discussion

We report a novel, cell-based functional assay of  $G_s$ - or  $G_i$ -coupled GPCR modulators based on cAMP-dependent activation of CFTR  $Cl^-$  channels. The assay is technically simple, inexpensive, and readily adaptable to fluorescence-based, high-throughput screening formats. The assay used an epithelial cell line suitable for both fluorescence and electrophysiological measurements. The cells have low basal halide conductance and cAMP concentration, excellent transfection efficiency, and rapid growth on uncoated plastic. The  $Z'$  factor for the assay was  $\sim 0.7$ , indicating very good sensitivity and specificity in a single primary screen. The assay was applied to identify  $V_2R$  antagonists in a screen of 50,000 small molecules in a 96-well plate format. Our assay was designed as a "pathway screen," so that compounds inhibiting CFTR  $I^-$  influx could function as  $V_2R$  antagonists,  $G_s$  inhibitors,  $G_i$  activators, adenylyl cyclase inhibitors, phosphodiesterase activators, protein kinase A inhibitors, or CFTR inhibitors. Such a pathway screen has the advantage of identifying small-molecule modulators of multiple targets in a single screen, with target identification done in small-scale secondary assays.

Functional assays of cell responses are widely used in high-throughput screening, in part because they are technically easier than radioligand binding assays. Binding assays are unable to distinguish between agonists and antagonists and have low sensitivity for the detection of allosteric modulators. Several functional assays have been developed based on cAMP measurement, as mentioned in the Introduction. An advantage of the standard cAMP antibody competitive

assay is that it does not require the generation of a stable cell line if cells are available with endogenous expression of the GPCR of interest. Disadvantages of this assay include the long incubations with cAMP antibody, the need for multiple washing steps, and the relatively high cost. Reporter gene assays, using green fluorescent protein, luciferase, or  $\beta$ -lactamase, are generally more sensitive than competition assays, in part because reporter transcription is downstream from cAMP, which can produce effective signal amplification. However, disadvantages of reporter gene assays include the requirement of a stable cell line expressing a reporter gene driven by a cAMP response element and long incubation time for transcription, in which receptor down-regulation can occur. In addition, for some reporter assays cell lysis is required, and costly signal-producing reagents are needed. The functional assay described here is suitable for discovery of modulators of  $G_s$ - or  $G_i$ -coupled GPCRs. Our assay is homogeneous and very sensitive and requires only three handling steps before measurement. The assay does not require lysis or reagent addition steps. The total cost of medium, reagents, and disposable supplies is  $\sim \$4$  (U.S.) per 96-well plate. However, our assay does require a specialized cell line expressing CFTR, YFP, and the GPCR of interest. To our knowledge, the only assay of this general type was developed by Atto Bioscience (Rich and Karpen, 2005), in which calcium influx was used as a readout of cyclic nucleotide-sensitive ion channels.

Our study applied the GPCR pathway screen to identify inhibitors of vasopressin-stimulated cAMP acting through the  $V_2R$ . Clinical indications of  $V_2R$  antagonists include the treatment of hyponatremias associated with increased or

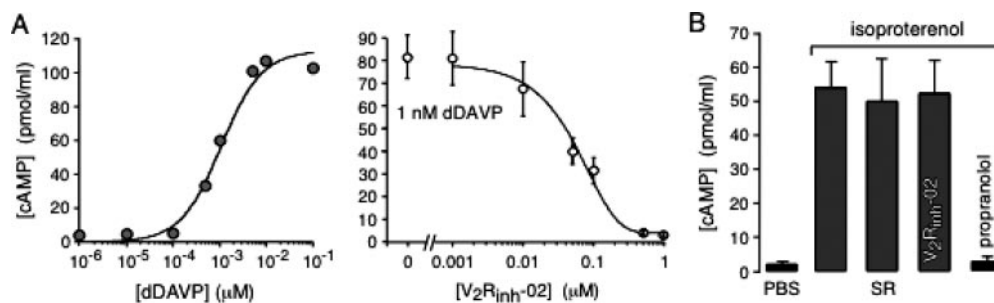


**Fig. 5.** Effects of  $V_2R_{inh-02}$  on cAMP concentration. A, left, cAMP concentration in FRT- $V_2R$  cells after 20-min incubation with various concentrations of dDAVP. Right, reduced cAMP after  $V_2R_{inh-02}$ . Cells were incubated for 20 min with 1 nM dDAVP and various concentrations of  $V_2R_{inh-02}$  (mean  $\pm$  S.E.,  $n = 3$ ). B, cAMP concentration in CHO cells transiently transfected with human  $\beta_2$ -adrenergic receptor. Cells were incubated for 20 min with 0.01  $\mu M$  isoproterenol in the presence of 20  $\mu M$  SR 121463A,  $V_2R_{inh-02}$ , or propranolol. The data are shown as mean  $\pm$  S.E.,  $n = 3$ .

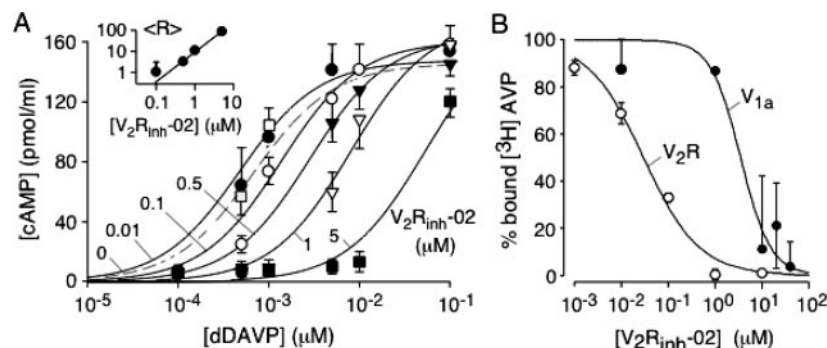


**Fig. 6.** Competitive binding and vasopressin receptor subtype selectivity of  $V_2R_{inh-02}$ . A, competition study showing cAMP concentration in FRT- $V_2R$  cells as a function of dDAVP concentration in the presence of indicated concentrations of  $V_2R_{inh-02}$  (mean  $\pm$  S.E.,  $n = 3$ ). Inset, Schild plot with slope of 1.3 and extrapolated  $K_i$  value of 70 nM. B, [ $^3H$ ]AVP binding displacement assays were done in intact FRT cells stably expressing  $V_2R$  or  $V_{1a}R$ . Cells were incubated for 2 h with 1 nM [ $^3H$ ]AVP in the presence of different concentration of  $V_2R_{inh-02}$ . Cell-associated radioactivity after incubation and washing (mean  $\pm$  S.E.,  $n = 3$ ). Nonspecific binding was subtracted. See *Materials and Methods* for details.

normal total body water, such as congestive heart failure, cirrhosis, and the syndrome of an inappropriate antidiuretic hormone secretion (Paranjape and Thibonnier, 2001). Water retention is a common clinical problem that increases the mortality and morbidity of underlying cardiovascular and hepatic diseases. The current main strategy in treating water retention is the use of diuretics, which increase excretion of both electrolytes and water. V<sub>2</sub>R antagonism causes an increase in water excretion without significant electrolyte loss and so is a superior treatment strategy. Early attempts to develop V<sub>2</sub>R antagonists focused on peptide analogs of vasopressin (Allison et al., 1988), although they had very low bioavailability. The first small-molecule V<sub>2</sub>R antagonist, OPC 31260, was a derivative of the vasopressin V<sub>1a</sub> receptor antagonist OPC 21268 (Thibonnier et al., 2001). A second V<sub>2</sub>R antagonist was SR 121463 (Serradeil-Le Gal et al., 1996). These V<sub>2</sub>R antagonists were originally identified by Otsuka Pharmaceutical Co. (Tokushima, Japan) and Sanofi, respectively. Both V<sub>2</sub>R antagonists have a diuretic effect in humans (Ohnishi et al., 1995; Serradeil-Le Gal, 2001), with IC<sub>50</sub> values in the nanomolar range. Then several pharmaceutical companies modified the structures of the original V<sub>2</sub>R antagonists to obtain more potent V<sub>2</sub>R antagonists (Yamamura et al., 1998; Gunnet et al., 2006), a dual V<sub>2</sub>R/V<sub>1a</sub>R antagonist (Tahara et al., 1997), and a V<sub>1b</sub>R antagonist (Serradeil-Le Gal et al., 2002). Only conivaptan (YM 087), a dual V<sub>2</sub>R/V<sub>1a</sub>R antagonist, has been approved for the treatment of euvolemic hyponatremia (Lemmens-Gruber and Kamyar, 2006). SR 121463, tolvaptan (OPC 41061), and lixivaptan (VPA 985) are in phase 3 clinical trials (Wong et al., 2003; Ghali et al., 2006; Schrier et al., 2006). However, the tricyclic antagonists are quite hydrophobic (logP >4) and have limited aqueous solubility (< 1 mg/ml) (Matthews et al., 2004), which are potentially problematic in further development for therapeutic purposes. New classes of V<sub>2</sub>R antagonists could provide useful lead compounds that might overcome these concerns.

Our small-molecule screen of 50,000 compounds identified a novel chemical class of V<sub>2</sub>R antagonists that are unrelated to known V<sub>2</sub>R antagonists. Seventy percent of the compounds identified by the primary screening were confirmed in the secondary screening. The failure to add dDAVP by the robotic system because of the clogged pipette tips might account for these false positives. After confirming the class of 5-aryl-4-benzoyl-3-hydroxy-1-(2-arylethyl)-2H-pyrrol-2-one were bona fide V<sub>2</sub>R antagonists, a small screen of commercially available structural analogs was done, identifying V<sub>2</sub>R<sub>inh</sub>-02 as the most potent compound of the 3-hydroxy-2-pyrrolones. Comparing the structure of the active and inactive compounds gave insight to the structural determinants of compound activity. In general, R<sub>1</sub> tolerated various substituted phenyl rings, R<sub>2</sub> was more limited in the fact that primarily 4-halophenyl and 4-nitrophenyl derivatives gave active compounds, and R<sub>3</sub> tolerated phenyl and 4-hydroxyphenyl substitution. A more focused 3-hydroxy-2-pyrrolone library incorporating the functional groups of the most active V<sub>2</sub>R<sub>inh</sub>-02 antagonists and having more diversity in R<sub>1</sub> and R<sub>3</sub> should yield more potent V<sub>2</sub>R antagonists and compounds with different V<sub>2</sub>R versus V<sub>1</sub>R selectivities.

Although the displacement assay of radiolabeled vasopressin cannot distinguish between competitive and allosteric antagonists, it did confirm that V<sub>2</sub>R<sub>inh</sub>-02 was a V<sub>2</sub>R antag-

onist. V<sub>2</sub>R<sub>inh</sub>-02 was found to be a competitive antagonist of dDAVP/vasopressin binding to the V<sub>2</sub>R, as demonstrated in cAMP measurements after cell incubations with different V<sub>2</sub>R<sub>inh</sub>-02/dDAVP concentrations. The existing, chemically unrelated V<sub>2</sub>R antagonists OPC 31260 and SR 121463 are also competitive antagonists (Serradeil-Le Gal et al., 1996; Thibonnier et al., 2001). The K<sub>i</sub> value of V<sub>2</sub>R<sub>inh</sub>-02 was ~70 nM, as estimated from competition data. V<sub>2</sub>R<sub>inh</sub>-02 was ~70 times more selective for V<sub>2</sub>R than V<sub>1a</sub>, as demonstrated by radioactive binding assay.

In conclusion, we have established a novel high-throughput screening pathway assay for the identification of modulators of G<sub>s</sub> or G<sub>i</sub>-coupled GPCRs. The assay is very sensitive, technically simple, and inexpensive compared with existing cell-based GPCR assays. The 5-aryl-4-benzoyl-3-hydroxy-1-(2-arylethyl)-2H-pyrrol-2-one V<sub>2</sub>R antagonists discovered in a small-molecule screen using the assay have favorable properties to support their further evaluation for aquaretic therapy.

#### Acknowledgments

We thank Baoxue Yang, Chatchai Muanprasat, Samira Saadoun, and Mariko Hara Chikuma for advice and technical support.

#### References

- Aliev ZG, Maslivets AN, Bannikova YN, and Atovmyan LO (2003) Interaction of 1-benzyl-4-benzoyl-5-phenyl-2,3-dihydro-2,3-pyrroledione with ketene diethylacetal: synthesis and crystal and molecular structure of 1-benzyl-4-benzoyl-3-hydroxy-5-phenyl-5-ethoxycarbonylmethyl-2,5-dihydro-2-pyrrolone. *J Struct Chem* **44**:707–710.
- Allison NL, Albrightson-Winslow CR, Brooks DP, Stassen FL, Huffman WF, Stote RM, and Kinter LB (1988) Species heterogeneity and antidiuretic hormone antagonists: what are the predictors? in *Vasopressin: Cellular and Integrative Functions* (Cowley AW, Liard J-F, and Ausiello DA eds) pp 207–214, Raven Press Ltd., New York.
- Chalmers DT and Behan DP (2002) The use of constitutively active GPCRs in drug discovery and functional genomics. *Nat Rev Drug Discov* **1**:599–608.
- Chang CT, Bens M, Hummler E, Boukroun S, Schild L, Teulon J, Rossier BC, and Vandewalle A (2005) Vasopressin stimulated CFTR chloride currents are increased in the renal collecting duct cells of a mouse model of Liddle's syndrome. *J Physiol* **562**:271–284.
- Galiotta LJ, Haggie PM, and Verkman AS (2001a) Green fluorescent protein-based halide indicators with improved chloride and iodide affinities. *FEBS Lett* **499**:220–224.
- Galiotta LJ, Jayarama S, and Verkman AS (2001b) Cell based assay for high throughput quantitative screening of CFTR chloride transport agonists. *Am J Physiol Cell Physiol* **281**:C1734–C1742.
- Ghali JK, Koren MJ, Taylor JR, Brooks-Asplund E, Fan K, Long WA, and Smith N (2006) Efficacy and safety of oral Conivaptan: a V<sub>1a</sub>/V<sub>2</sub> vasopressin receptor antagonist, assessed in a randomized, placebo-controlled trial in patients with euvolemic or hypervolemic hyponatremia. *J Clin Endocrinol Metab* **91**:2145–2152.
- Gunnet JW, Matthews JM, Maryanoff BE, Garavilla LD, Andrade-Gordon P, Damiano B, Hageman W, Look R, Stahle P, Streeter AJ, et al. (2006) Characterization of RWJ-351647, a novel, nonpeptide vasopressin V<sub>2</sub> receptor antagonist. *Clin Exp Pharmacol Physiol* **33**:320–326.
- Hill SJ (2001) Reporter-gene systems for the study of GPCRs. *Curr Opin Pharmacol* **1**:526–532.
- Hill SJ (2006) G-protein-coupled receptors: past, present and future. *Br J Pharmacol* **147**:S27–S37.
- Hopkins AL and Groom CR (2002) The druggable genome. *Nat Rev Drug Discov* **1**:727–730.
- Horstman DA, Takemura H, and Putney JW Jr (1988) Formation and metabolism of [<sup>3</sup>H]inositolphosphates in AR42J pancreatoma cells. Substance P-induced Ca<sup>2+</sup> mobilization in the apparent absence of inositol 1,4,5-triphosphate 3-kinase activity. *J Biol Chem* **263**:15297–15303.
- Innamorati G, Sadeghi H, and Birnbaumer M (1996) A fully active non glycosylated V<sub>2</sub> vasopressin receptor. *Mol Pharmacol* **50**:467–473.
- Kenakin T (1997) Competitive antagonism, in *Pharmacologic Analysis of Drug Receptor Interaction*, 3rd ed, pp 331–373, Lippincott-Raven, Philadelphia.
- Lemmens-Gruber R and Kamyar M (2006) Vasopressin antagonists. *Cell Mol Life Sci* **63**:1766–1779.
- Ma T, Thiagarajah JR, Yang H, Sonawane ND, Folli C, Galiotta LJ, and Verkman AS (2002) Thiazolidinone CFTR inhibitor identified by high throughput screening blocks cholera toxin-induced intestinal fluid secretion. *J Clin Invest* **110**:1651–1658.
- Manning M, Cheng LL, Stoev S, Klis W, Nawracka E, Olma A, Sawyer WH, Wo NC, and Chan WY (1997) Position three in vasopressin antagonist tolerates conformationally restricted and aromatic amino acid substitutions: a striking contrast with vasopressin agonists. *J Pept Sci* **3**:31–46.

- Matthews JM, Hoekstra WJ, Dyatkin AB, Hecker LR, Hlasta DJ, Poulter BL, Andrade-Gordon P, Gsravilla L, Demarest KT, Ericson E, et al. (2004) Potent nonpeptide vasopressin receptor antagonists based on oxazino- and thiazinobenzodiazepine templates. *Bioorg Med Chem Lett* **14**:2747–2752.
- Monteith GR and Bird GS (2005) Techniques: high-throughput measurement of intracellular  $Ca^{2+}$  back to basics. *Trends Pharmacol Sci* **26**:218–223.
- Muanprasat C, Sonawane ND, Salinas D, Taddei A, Galiotta LJ, and Verkman AS (2004) Discovery of glycine hydrazone pore occluding CFTR inhibitors: mechanism, structure-activity analysis, and in vivo efficacy. *J Gen Physiol* **124**:125–137.
- Ohnishi A, Orita Y, Takagi N, Fujita T, Toyoki T, Ihara Y, Yamamura Y, Inoue T, and Tanaka T (1995) Aquaretic effect of a potent, orally active, non-peptide  $V_2$  antagonist in man. *J Pharmacol Exp Ther* **272**:546–551.
- Oksche A, Schulein R, and Rutz C (1996) Vasopressin  $V_2$  receptor mutants that cause x-linked nephrogenic diabetes insipidus: analysis of expression, processing, and function. *Mol Pharmacol* **50**:820–828.
- Paranjape SB and Thibonnier M (2001) Development and therapeutic indications of orally active non-peptide vasopressin receptor antagonists. *Expert Opin Investig Drugs* **10**:825–834.
- Pedemonte N, Lukacs GL, Du K, Caci E, Zegarra-Moran O, Galiotta LJ, and Verkman AS (2005) Small molecule correctors of defective  $\Delta F508$ -CFTR cellular processing identified by high-throughput screening. *J Clin Invest* **115**:2564–2571.
- Rich TC and Karpen JW (2005) High-throughput screening of phosphodiesterase activity in living cells. *Methods Mol Biol* **307**:45–61.
- Robben JH, Knoers NV, and Deen PM (2004) Regulation of the vasopressin  $V_2$  receptor by vasopressin in polarized renal collecting duct cells. *Mol Biol Cell* **15**:5693–5699.
- Sadeghi HM, Innamorati G, Dagarag M, and Birnbaumer M (1997) Palmitoylation of the  $V_2$  vasopressin receptor. *Mol Pharmacol* **52**:21–29.
- Saito M, Tahara A, and Sugimoto T (1997) 1-desamino-8-D-arginine vasopressin (dDAVP) as an agonist on  $V_1b$  vasopressin receptor. *Biochem Pharmacol* **53**:1711–1717.
- Schrier RW, Gross P, Gheorghiane M, Berl T, Verbalis JG, Czerwiec FS, Orlandi C, and SALT Investigators (2006) Tolvaptan, a selective oral vasopressin  $V_2$ -receptor antagonist, for hyponatremia. *N Engl J Med* **355**:2099–2112.
- Seethala R and Fernandes B (2001) Assay miniaturization: developing technologies and assay formats, in *Handbook of Drug Screening*, pp 550–553, Marcel Dekker, New York.
- Serradeil-Le Gal C (2001) An overview of SR121463, a selective non-peptide vasopressin  $V_2$  receptor antagonist. *Cardiovasc Drug Rev* **19**:201–214.
- Serradeil-Le Gal C, Lacour C, Valette G, Garcia G, Foulon L, Galindo G, Bankir L, Pouzet B, Guillon G, Barberis C, et al. (1996) Characterization of SR 121463A, a highly potent and selective, orally active vasopressin  $V_2$  receptor antagonist. *J Clin Invest* **98**:2729–2738.
- Serradeil-Le Gal C, Wagnon J, Garcia C, Lacour C, Guiraudou P, Christophe B, Villanova G, Nisato D, Maffrand JP, and Le Fur G (1993) Biochemical and pharmacological properties of SR 49059, a new, potent, non peptide antagonist of rat and human  $V_{1a}$  receptors. *J Clin Invest* **92**:224–231.
- Serradeil-Le Gal C, Wagnon J, Simiand J, Griebel G, Lacour C, Guillon G, Barberis C, Brossard G, Soubrie P, Nisato D, et al. (2002) Characterization of (2S,4R)-1-[5-chloro-1-[(2,4-dimethoxyphenyl)sulfonyl]-3-(2-methoxy-phenyl)-2-oxo-2,3-dihydro-1H-indol-3-yl]-4-hydroxy-N,N-dimethyl-2-pyrrolidinecarboxamide (SSR149415), a selective and orally active vasopressin  $V_{1b}$  receptor antagonist. *J Pharmacol Exp Ther* **300**:1122–1130.
- Tahara A, Tomura Y, Wada KI, Kusayama T, Tsukada J, Takanashi M, Yatsu T, Uchida W, and Tanaka A (1997) Pharmacological profile of YM087, a novel potent non-peptide vasopressin  $V_{1a}$  and  $V_2$  receptor antagonist, in vitro and in vivo. *J Pharmacol Exp Ther* **282**:301–308.
- Thibonnier M, Coles P, Thibonnier A, and Shoham M (2001) The basic and clinical pharmacology of non-peptide vasopressin receptor antagonists. *Annu Rev Pharmacol Toxicol* **41**:175–202.
- Williams C (2004) cAMP detection methods in high throughput screening: selecting the best from the rest. *Nat Rev Drug Discov* **3**:125–135.
- Wise A, Jupe SC, and Rees S (2004) The identification of ligands at orphan G protein coupled receptors. *Annu Rev Pharmacol Toxicol* **44**:43–66.
- Wong F, Blei AT, Blendis LM, and Thuluvath PJ (2003) A vasopressin receptor antagonist (VPA-985) improves serum sodium concentration in patients with hyponatremia: a multicenter, randomized, placebo-controlled trial. *Hepatology* **37**:182–191.
- Yamamura Y, Nakamura S, Itoh S, Hirano T, Onogawa T, Yamashita T, Yamada Y, Tsujimae K, Aoyama M, Kotosai K, et al. (1998) OPC-41061, a highly potent human vasopressin  $V_2$  receptor antagonist: pharmacological profile and aquaretic effect by single and multiple oral dosing in rats. *J Pharmacol Exp Ther* **287**:860–867.

---

**Address correspondence to:** Dr. Alan S. Verkman, 1246 Health Sciences East Tower, Box 0521, University of California, San Francisco, CA 94143-0521. E-mail: alan.verkman@ucsf.edu

---